LARGE SCALE STRUCTURE OF THE UNIVERSE: CURRENT PROBLEMS

J. EINASTO
Tartu Observatory, EE-61602 Tõravere, Estonia

I compare the mean power spectrum of galaxies with theoretical models and discuss possibilities to explain the observed power spectrum. My principal conclusion is that some of the presently accepted cosmological paradigms need revision if the available observational data represent a fair sample of the Universe.

1 Introduction

According to current paradigms the Universe is homogeneous and isotropic on large scales, density perturbations grow from small random fluctuations generated in the early stage of the evolution (inflation), and the dynamics of the Universe is dominated by cold dark matter (CDM) with some possible mixture of hot dark matter (HDM). On small scales galaxies are associated in groups and clusters. Until recently it was assumed that the homogeneity of the Universe starts on scales above 50 h_{100}^{-1} Mpc. However, there is growing evidence that the supercluster-void network has some regularity, and that homogeneity occurs on larger scales only. Broadhurst *et al.* (1990) measured redshifts of galaxies in a narrow beam towards the northern and southern Galactic poles and found that the distribution is periodic: high-density regions (which indicate superclusters of galaxies, see Bahcall 1991) alternate with low-density ones (voids) with a surprisingly constant interval of $\approx 128\ h_{100}^{-1}$ Mpc (here h is the Hubble constant in units of 100 km s^{-1} Mpc^{-1}). The distribution of galaxies in this beam can be characterized by a power spectrum which has a sharp peak. The power spectra derived on the basis of large cluster samples have maxima around the same scale (Einasto *et al.* 1997a, 1999a). Below we shall analyze observed power spectra of galaxies and clusters of galaxies and compare them with theoretical spectra found for various models.

2 The power spectrum of galaxies and its interpretation

We have analyzed recent determinations of power spectra of large galaxy and cluster samples. The mean power spectrum found from cluster samples (Einasto *et al.* 1997c, Retzlaff *et al.* 1998, Tadros *et al.* 1998) and the APM 3-D galaxy sample (Tadros and Efstathiou 1996) has a relatively sharp maximum at wavenumber $k = 0.05\ h$ Mpc^{-1}, which corresponds to a scale of

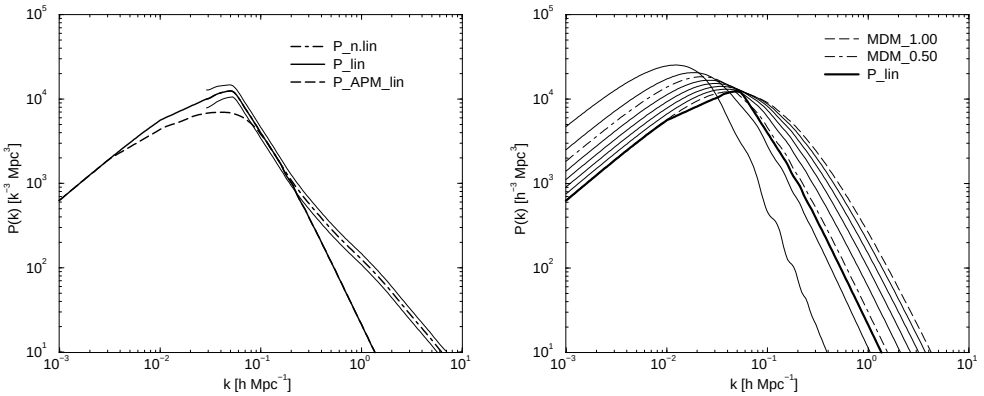

Figure 1. The left panel shows empirical power spectra of matter. $P_{n.lin}$ is the non-linear power spectrum of matter with its 1σ error corridor; P_{lin} and $P_{APM-lin}$ are the linear power spectra for empirical spectra derived from large cluster samples and from the APM 2-D galaxy sample (Peacock 1997, Gaztañaga & Baugh 1998), respectively. The right panel gives the empirical linear power spectrum of matter compared with theoretical spectra for MDM models with $\Omega_0 = 1.0,\ 0.9, \ldots\ 0.4,\ 0.25$; for clarity the models with $\Omega_0 = 1.0$ and $\Omega_0 = 0.5$ are drawn as dashed lines.

120 h_{100}^{-1} Mpc, and an almost exact power law with index $n = -1.9$ on scales shorter than the maximum. In contrast, the power spectrum found from deprojection of the 2-D distribution of APM galaxies (Peacock 1997, Gaztañaga & Baugh 1997) is shallower around the maximum, see Figure 1. We may expect that true 3-D and deeper surveys reflect better the actual distribution of galaxies and clusters, thus we assume that the power spectrum based on cluster data is characteristic for all galaxies in a fair sample of the Universe (Einasto *et al.* 1999a,b). The spectrum is derived in real space, then reduced to the amplitude of the spectrum of matter, and finally corrected for non-linear effects; it is determined from observations on scales $\leq 200\ h_{100}^{-1}$ Mpc, while on very large scales it is extrapolated using theoretical model spectra.

In the right panel of Figure 1 we compare the empirical power spectrum with theoretical models. The best agreement is achieved with a mixed dark matter (MDM) model with cosmological constant. We have accepted parameters of models in agreement with recent data: Hubble constant $h = 0.6$; baryon density $\Omega_b = 0.04$ (this gives $\Omega_b h^2 = 0.0144$); hot dark matter density $\Omega_\nu = 0.1$. We use spatially flat models with cosmological constant, $\Omega_0 + \Omega_\Lambda = 1$. The matter density $\Omega_0 = \Omega_b + \Omega_c + \Omega_\nu$ was varied between 1.0 and 0.25, the cold dark matter fraction Ω_c and vacuum energy term Ω_Λ were chosen in agreement with restrictions given above. The amplitude of

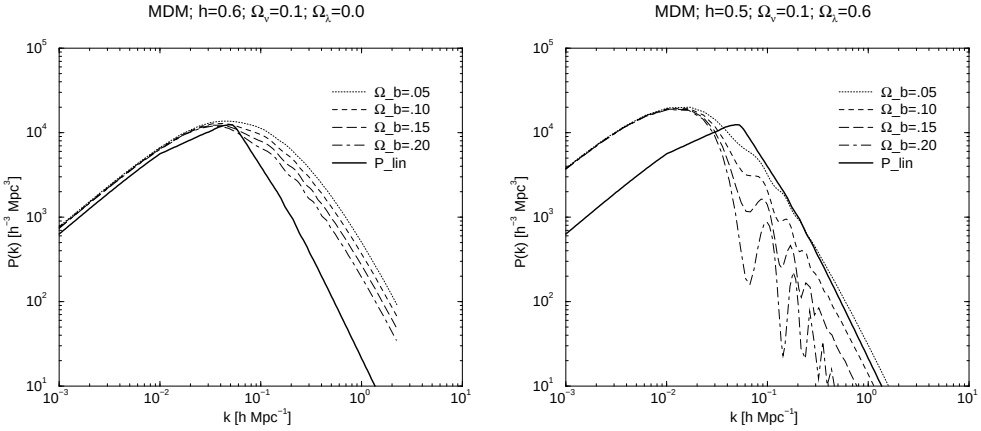

Figure 2. The empirical linear power spectrum of matter compared with theoretical spectra for MDM models of variable baryon density. Left panel shows model spectra with zero vacuum energy density, right panel with $\Omega_\Lambda = 0.6$.

power spectra on large scales was normalized using four-year COBE data. All models are based on the basic assumption that the primordial power spectrum is a power law; we have calculated model spectra for power indices of 1.0, 1.1, ... 1.4; model spectra plotted in Figure 1 were derived for $n = 1.0$.

Figure 1 shows that on scales shorter than the scale of the maximum the best agreement with observations is obtained with a model with density parameter $\Omega_0 \approx 0.4$. By fine tuning the density parameter Ω_0 and power index n it is possible to get an almost exact representation of the empirical power spectrum on scales $< 120\ h_{100}^{-1}$ Mpc. The agreement is lost on large scales. The power spectra of models with low density value continue to rise toward large scales as seen in Figure 1. An agreement with the amplitude of theoretical power spectra is possible only for models with high density parameter, $\Omega_0 \approx 1$. However, models with high density parameter have amplitudes much higher than the empirical spectrum. It is impossible to satisfy the shape of the empirical power spectrum with models with any fixed density parameter simultaneously on large and small scales. This is the main conclusion obtained from the comparison of cosmological models with the data. The main reason for this disagreement is that the empirical power spectrum is narrower: its full width at half height of the maximum is about 0.8 dex, whereas conventional CDM models have this parameter in the range $1.10 - 1.26$ dex, and MDM models in the range $1.00 - 1.15$ dex (lower value for lower density parameter).

One possibility to explain this discrepancy and to decrease the width of

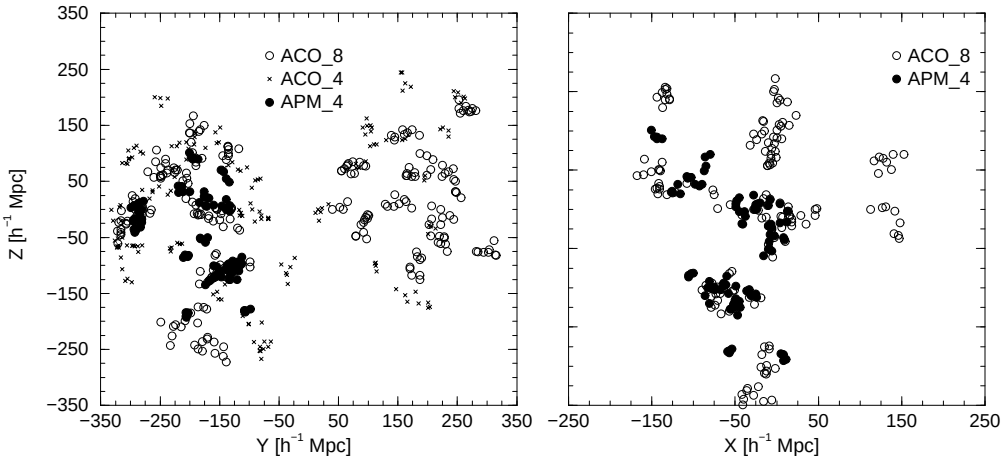

Figure 3. Distribution of clusters in high-density regions in supergalactic coordinates. Left panel shows clusters in a sheet in supergalactic $-100 \leq X \leq 200\ h_{100}^{-1}$ Mpc; Abell-ACO and APM clusters in superclusters with at least 8 or 4 members are plotted with symbols as indicated. The supergalactic $Y = 0$ plane coincides almost exactly with the Galactic equatorial plane and marks the Galactic zone of avoidance. In the right panel only clusters in the southern Galactic hemisphere are plotted; here the depth is $-350 \leq Y \leq -50\ h_{100}^{-1}$ Mpc.

the power spectrum is to increase the baryon fraction in the cosmic density budget (Eisenstein *et al.* (1998) and Meiksin, White & Peacock (1999)). In this case the amplitude of Sakharov oscillations of the hot plasma before recombination increases which decreases the width of the power spectrum and increases the amplitude of the power spectrum near the peak. We have checked this possibility and calculated the power spectra for a range of baryon densities, varying also the Hubble parameter and vacuum energy density (cosmological constant term). Figure 2 shows results for a set of MDM models with Hubble constant $h = 0.5$ and $h = 0.6$, vacuum energy density $\Omega_\Lambda = 0.0$ and 0.6, and HDM fraction $\Omega_\nu = 0.1$, the baryon density was varied between 0.05 and 0.20. The increase of the baryon fraction in models with high cosmological density (and zero cosmological constant) does not change the power spectrum considerably – the width of the spectrum remains too large. In models with large cosmological constant an increase of the baryon fraction decreases the width of the power spectrum, however, Sakharov oscillations of the spectrum become too large. Moreover, the shape of all theoretical power spectra is very different from the shape of empirical spectra. The first peak of Sakharov oscillations occurs on a scale of $k \approx 0.1\ h$ Mpc^{-1}; the location of the overall maximum of the power spectrum depends on the density parameter.

For low-density models it is located near $k \approx 0.01\ h$ Mpc^{-1}, the observed maximum lies in-between. Varying the Hubble constant does not change the overall picture, and there remain essential differences between models and data.

Thus our calculations show that no combination of cosmological parameters enables us to obtain a good representation of the empirical power spectrum with theoretical models which are based on the assumption that the primordial power spectrum is a single power law. There remain two possibilities, either empirical data are in error or the single power law assumption is wrong.

3 Geometry of the distribution of clusters

Consider first the possibility that the observed power spectrum is not accurate enough, and that there is actually no discrepancy between models and data. Differences occur on scales near the maximum of the spectrum. Here density perturbations have the largest amplitudes, thus it is clear that maxima correspond to superclusters – large-scale regions of highest density in the Universe, and minima to large voids between superclusters – regions of lowest overall density. Differences in power spectra on these scales reflect differences in the spatial distribution of superclusters and voids. To understand the meaning of differences between observed and theoretical power spectra we shall compare the distribution of real and model superclusters and voids. The most suitable objects to investigate the distribution of superclusters are rich clusters of galaxies.

Figure 3 presents the distribution of Abell-ACO and APM clusters of galaxies located in rich superclusters with at least 4 or 8 member clusters (Toomet *et al.* 1999). To emphasize the distribution of regions of highest density, which define the power spectrum near the maximum, we plot only clusters in rich superclusters. Figure 3 shows that the distribution of rich clusters is quasi-regular: superclusters and voids form a honeycomb-like pattern. The diameter of a cell in this network is approximately 120 h_{100}^{-1} Mpc, which is very close to the scale of the maximum of the power spectrum.

In contrast to the observed case the distribution of rich superclusters in CDM dominated models is almost random (Frisch *et al.* 1995). Mock catalogues with randomly distributed superclusters have power spectra with broad maxima similar to spectra of CDM-type models (Einasto *et al.* 1997b). The presence of broad maxima is an intrinsic property of all CDM-type models (if the baryon fraction is not too high).

The distribution of clusters can also be quantified using the correlation

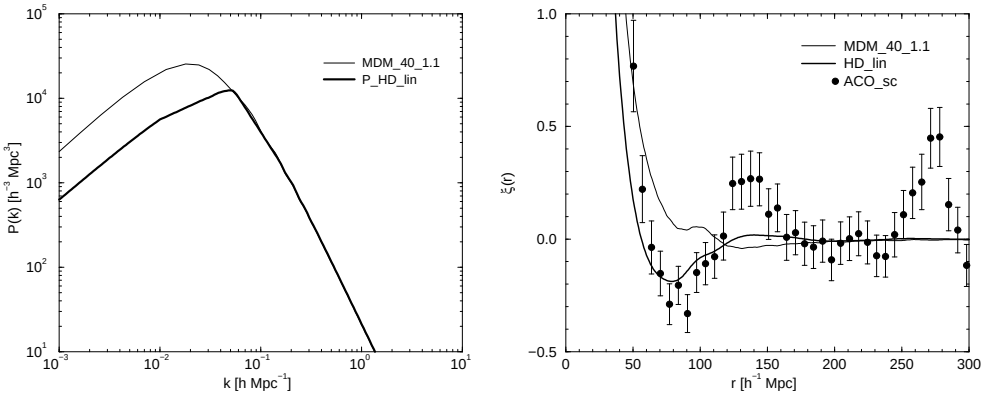

Figure 4. Power spectrum (left) and correlation function (right) of the MDM model with density parameter $\Omega_0 = 0.4$, compared with the linear empirical power spectrum of matter and correlation function of clusters of galaxies in rich superclusters. The power spectrum of the MDM model is calculated with spectral index $n = 1.1$. Cluster correlation functions are calculated via Fourier transform from power spectra of matter, and are enhanced in amplitude by a biasing factor 7.7 which corresponds to the mean difference between respective power spectra. The observed cluster correlation function is the one for Abell-ACO clusters in very rich superclusters as derived by E97b.

function of clusters of galaxies. While on small scales the correlation function characterizes the distribution of clusters within superclusters, on large scales it describes the distribution of superclusters themselves (Einasto *et al.* 1997a, 1999b). In Figure 4 we compare power spectra and correlations functions of the MDM model for a density parameter $\Omega_0 = 0.4$ with respective empirical data. We use the observed correlation function of clusters of galaxies located in rich superclusters, and for comparison the Fourier transform of the empirical power spectrum of matter, enhanced in amplitude to obtain a correlation function comparable with the function for rich superclusters. The observed correlation function of clusters in rich superclusters is oscillating with a period equal to the wavelength of the maximum of the power spectrum. The Fourier transform of the empirical power spectrum has a similar property, only that the amplitude of oscillations is lower. The reason for this difference is due to the elongated form of the cluster sample which enhances the amplitude of oscillations at large separations. These oscillations are due to quasi-regular distribution of rich superclusters seen in Figure 3. The correlation function calculated for the MDM model has a completely different character on large scales, and corresponds to an almost random distribution of rich superclusters.

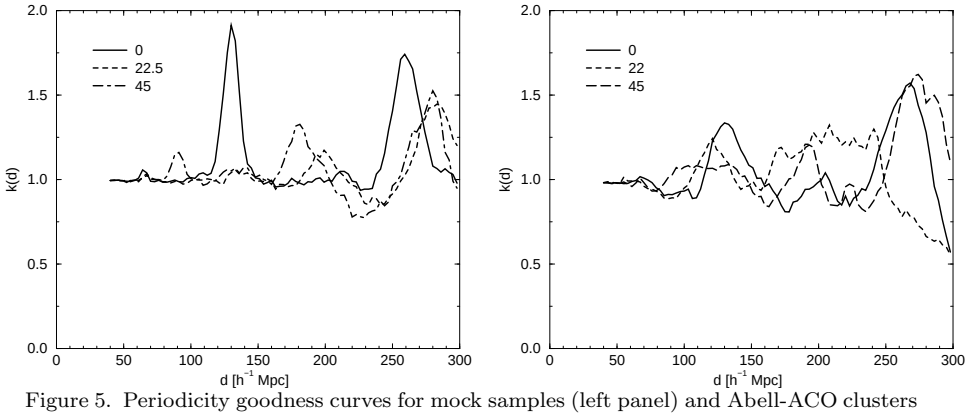

Figure 5. Periodicity goodness curves for mock samples (left panel) and Abell-ACO clusters (right panel). Mock samples have 300 randomly located clusters and 100 clusters in quasi-regularly located superclusters. The step of the regular grid is $r_0 = 130\ h_{100}^{-1}$ Mpc; samples are cubical. In both panels solid, dashed and dot-dashed lines are for trial cubes oriented at 0°, 22.5° and 45° with respect to the main symmetry axis of the mock sample, and with respect to supergalactic coordinates of the real sample.

Finally, to describe the regularity of the cluster distribution we use a novel method which is sensitive to the geometry of the distribution (Toomet *et al.* 1999). The method is a 3-D generalization of the periodicity analysis of time series of variable stars. The space under study is divided into cubical trial cells of side length d. All objects in the individual cubical cells are stacked to a single combined cell, preserving their phases in the original cells. We then vary the side-length of the trial cube to search for the periodicity of the cluster distribution. We find the goodness of regularity for the side length d of the trial cell; it is defined so that it has a maximum > 1 if the length of the trial cell is equal to the period of the regularity, otherwise it is equal to unity. The goodness of regularity is shown in Figure 5, the left panel gives results for a mock catalogue (see Figure caption), the right panel for the actual Abell-ACO cluster sample.

The method is sensitive to the direction of the axes of the trial cubes. If clusters form a quasi-rectangular cellular network, and the search cube is oriented along the main axis of the network, then the period is found to be equal to the side-length of the cell. If the search cube is oriented at some non-zero angle in respect to the major axis of the network, then the presence of the periodicity and the period depend on the angle. If the angle is $\approx 45°$, then the period is equal to the length of the diagonal of the cell. If the angle

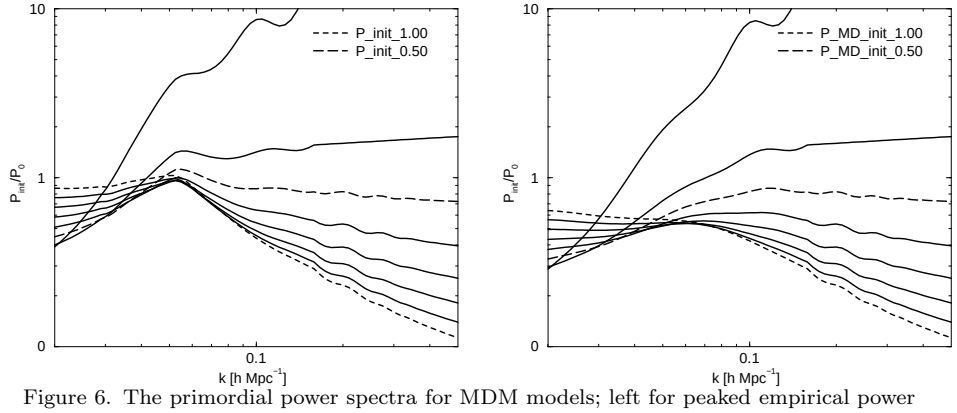

Figure 6. The primordial power spectra for MDM models; left for peaked empirical power spectra, right for shallower spectra derived from APM 2-D galaxy data. Primordial power spectra are divided by the scale-free spectrum, $P(k) \sim k$. Spectra are found for theoretical transfer functions with $\Omega_0 = 1.0,\ 0.9, \ldots\ 0.25$; for clarity the spectra for models with $\Omega_0 = 1.0$ and $\Omega_0 = 0.5$ are drawn with dashed lines.

differs considerably from 0° and 45°, the periodicity is weak or absent. As seen from Figure 5, the main axis of the supercluster-void network is approximately oriented toward supergalactic coordinates. As the supergalactic Y axis is very close to the direction of the Galactic poles, it is natural to expect a well defined periodicity in these directions as really observed by Broadhurst *et al.* (1990). Our periodicity analysis confirms earlier results on the presence of a high concentration of clusters and superclusters towards both the Supergalactic Plane (Tully *et al.* 1992), and towards the Dominant Supercluster Plane, which are oriented at right angles with respect to each other (Einasto *et al.* 1997d).

4 Primordial power spectra

Previous analysis has shown that there exist essential differences between data and CDM-type models with scale-free primordial power spectra. To explain the difference between model and data we have to accept a non-conventional theoretical power spectrum. As we have presently no reason to assume that our understanding of physical processes during the radiation domination era is wrong, we suppose that the peaked power spectrum originated during the earliest inflational phase of the evolution of the Universe. If we accept the transfer function (which describes the evolution of the power spectrum during

the radiation domination era) according to models described above, we derive the primordial power spectrum shown in Figure 6 (Einasto *et al.* 1999b).

The main features of primordial power spectra are the presence of a spike and the change of the power index at the same scale as that of the maximum of the empirical power spectrum. On scales shorter or larger than that of the spike, the primordial spectrum can be well approximated by a power law. The power indices of the approximation are different on small and large scales. Both alternative empirical power spectra lead to similar primordial power spectra, only the shape around the break is different. Broken-scale-invariant primordial power spectra have been studied by Starobinsky (1992), Adams, Ross & Sarkar (1997), and Lesgourgues *et al.* (1998), among others. It is too early to say which of these models describes the observational data better.

5 Conclusions

Our main conclusions are:

• The empirical power spectrum of matter has a peak on scales near 120 h_{100}^{-1} Mpc; on shorter scales it can be approximated by a power law with index $n = -1.9$.

• Superclusters and voids form a quasi-regular lattice of mean cell size 120 h_{100}^{-1} Mpc; the main axis of the lattice is directed toward the supergalactic Y coordinate.

• On scales around 100 h_{100}^{-1} Mpc the Universe is neither homogeneous nor isotropic.

• The primordial power spectrum of matter is broken, its effective power index changes around the scale $\approx 120\ h_{100}^{-1}$ Mpc.

I thank H. Andernach, F. Atrio-Barandela, M. Einasto, E. Kasak, A. Knebe, V. Müller, A. Starobinsky, E. Tago, O. Toomet and D. Tucker for fruitful collaboration and permission to use our joint results in this review article. This study was supported by the Estonian Science Foundation.

References

1. Adams, J.A., Ross, G.G., & Sarkar, S. 1997, Nucl. Phys. B503, 405, hep-ph/9704286
2. Bahcall N. A., 1991, ApJ 376, 43
3. Broadhurst, T. J., Ellis, R. S., Koo, D. C., and Szalay, A. S., 1990, Nature, 343, 726

4. Einasto, J., Einasto, M., Frisch, P., Gottlöber, S., Müller, V., Saar, V., Starobinsky, A. A., Tago, E., Tucker, D., & Andernach, H., 1997a, MNRAS, 289, 801
5. Einasto, J., Einasto, M., Frisch, P., Gottlöber, S., Müller, V., Saar, V., Starobinsky, A. A., Tucker, D., 1997b, MNRAS, 289, 813
6. Einasto, J., Einasto, M., Gottlöber, S., Müller, V., Saar, V., Starobinsky, A. A., Tago, E., Tucker, D., Andernach, H., and Frisch, P., 1997c, Nature, 385, 139
7. Einasto, J., Einasto, M., Tago, E., Starobinsky, A.A., Atrio-Barandela, F., Müller, V., Knebe, A., Frisch, P., Cen, R., Andernach, H., & Tucker, D. 1999a, ApJ, 519, 441, astro-ph/9812247
8. Einasto, J., Einasto, M., Tago, E., Starobinsky, A.A., Atrio-Barandela, F., Müller, V., & Cen, R. 1999b, ApJ, 519, 469, astro-ph/9812249
9. Einasto, M., Tago, E., Jaaniste, J., Einasto, J., & Andernach, H., 1997d, A&AS, 123, 119
10. Eisenstein, D.J., Hu, W., Silk, J., & Szalay, A.S. 1998, ApJ, 494, L1
11. Frisch, P., Einasto, J., Einasto, M., Freudling, W., Fricke, K.J., Gramann, M., Saar, V., & Toomet, O. 1995, A&A, 296, 611
12. Gaztañaga, E., and C. M. Baugh, C. M. 1997, MNRAS, 294, 229
13. Lesgourgues, J., Polarski, D. & Starobinsky, A.A. 1998, MNRAS, 297, 769
14. Meiksin, A., White, M., & Peacock (1999), MNRAS (submitted), astro-ph/9812214
15. Peacock, J. A., 1997, MNRAS, 284, 885
16. Retzlaff, J., Borgani, S., Gottlöber, S., Müller, V., 1998, NewA 3, 631
17. Starobinsky, A. A., 1992, J. Exper. Theor. Phys. Lett., 55, 489
18. Tadros, H., & Efstathiou, G. 1996, MNRAS, 282, 1381
19. Tadros, H., Efstathiou, G. & Dalton, G. 1998, MNRAS, 296, 995
20. Toomet, O., Andernach, H., Einasto, J., Einasto, M., Kasak, E., Starobinsky, & Tago, E., A&A, 1999 (submitted), astro-ph/9907238
21. Tully, R. B., Scaramella, R., Vettolani, G., Zamorani, G., 1992, ApJ, 388, 9.